

# Curcumin Alleviates Osteoarthritis Through the p38MAPK Pathway: Network Pharmacological Prediction and Experimental Confirmation

Xuan Wang<sup>1,\*</sup>, Hanjie Yu<sup>2,\*</sup>, Yunheng Zhang<sup>3,\*</sup>, Xin Chang<sup>1</sup>, Chengyi Liu<sup>1</sup>, Xiaodong Wen<sup>1</sup>, Feng Tian<sup>1</sup>, Yi Li<sup>1</sup>

<sup>1</sup>Department of Foot and Ankle Surgery, Honghui Hospital, Xi'an Jiaotong University, Xi'an, Shaanxi, People's Republic of China; <sup>2</sup>Laboratory for Functional Glycomics, College of Life Sciences, Northwest University, Xi'an, Shaanxi, People's Republic of China; <sup>3</sup>The Second Clinical Medical College, Shaanxi University of Chinese Medicine, Xianyang, Shaanxi, People's Republic of China

\*These authors contributed equally to this work

Correspondence: Yi Li, Email [liyidoctor@163.com](mailto:liyidoctor@163.com)

**Objective:** Osteoarthritis (OA) is a common degenerative disease worldwide. While curcumin has shown therapeutic effects on OA, its mechanism remains unknown. This study aimed to investigate the molecular mechanism of curcumin in treating OA through network pharmacology and both in vivo and in vitro experiments.

**Methods:** Curcumin-related targets were obtained using the HERB and DrugBank databases. GeneCards and DisGeNET were used to build a target database for OA. The STRING database was employed to construct protein-protein interaction networks and analyze related protein interactions. Kyoto Encyclopedia of Genes and Genomes (KEGG) pathway and gene ontology enrichment analyses of core targets were performed using Metascape. In addition, Autodock software was utilized for molecular docking validation of curcumin and disease targets. Further validation of the main findings was conducted through in vitro and in vivo experiments. In the in vitro experiments, an inflammation model was constructed through nitric oxide donor (SNP) stimulation of chondrocytes. Subsequently, the regulatory effects of curcumin on core targets and signaling pathways were validated using Western blotting and immunofluorescence staining techniques. In the in vivo experiments, an OA model was established by performing medial meniscectomy on male Sprague-Dawley rats. The therapeutic effects were evaluated using enzyme-linked immunosorbent assays, histologic staining, and micro-computed tomography (micro-CT) techniques.

**Results:** Core targets of curcumin relevant to OA therapy included tumor necrosis factor- $\alpha$  (TNF- $\alpha$ ), interleukin (IL)-1 $\beta$ , IL-6, matrix metalloproteinase 9 (MMP-9), B-cell lymphoma 2 (BCL-2), and caspase-3. The major biological processes involved oxidative stress and apoptotic processes, among others. The p38 mitogen-activated protein kinase (p38/MAPK) pathway was identified as the most likely pathway involved. In vitro experiments showed that curcumin significantly reduced oxidative stress levels, inhibited the expression of inflammatory factors IL-6 and Cyclooxygenase-2 (COX-2) and downregulated the expression of MMP-9 and MMP-1. In addition, curcumin was found to regulate the expression of BCL-2 and caspase-3 through the p38/MAPK pathway, inhibiting chondrocyte apoptosis. In vivo animal experiments demonstrated that curcumin significantly reduced the expression of OA-related factors (IL-1, IL-6, and TNF- $\alpha$ ). Histological analysis and micro-CT results revealed that curcumin treatment significantly increased cartilage thickness, improved cartilage morphology, structure, and function, inhibited cartilage degradation, and enhanced the resorption of subchondral bone in the knee joints of rats with OA.

**Conclusion:** Curcumin regulates oxidative stress and maintains mitochondrial function, thereby protecting chondrocyte guard. In addition, curcumin attenuates the inflammatory response of chondrocytes by inhibiting the phosphorylation of P38MAPK, slowing down the breakdown of the extrachondral matrix while preventing apoptosis of chondrocytes. Additionally curcumin attenuated cartilage degradation and bone damage while helping to boost bone density.

**Keywords:** osteoarthritis, curcumin, molecular mechanism, network pharmacology, p38/MAPK

## Introduction

Osteoarthritis (OA) is a degenerative disease that affects the health of middle-aged and older adults globally. The prevalence of OA has increased markedly due to the aging population and the rising obesity problem, adding substantially to the global healthcare burden.<sup>1</sup> Compared to the general population, patients with OA are at higher risk of all-cause mortality, particularly from cardiovascular disease. This excess mortality is closely associated with the degree of disability.<sup>2</sup> The manifestations of OA vary considerably among individuals, but they share some common features. For example, OA most commonly affects joints, including the knees, hands, hips, and spine, and it manifests through joint pain, impaired motion, tenderness, swelling, joint effusions, and localized inflammation.<sup>3</sup>

To date, the pathogenesis of OA remains unclear and is recognized as a complex and not fully elucidated process. OA can be categorized into primary and secondary types. Primary OA is associated with various risk factors, including wear and tear from joint motion, with the most prominent being aging and obesity. Secondary OA risk factors primarily include trauma, arthritic congenital malformations, and surgical sequelae.<sup>4</sup> The main features of OA include cartilage matrix degeneration, chondrocyte apoptosis, bone remodeling, and the formation of bone capillaries. Moreover, inflammatory factors are closely linked to the pathogenesis of OA, with various inflammatory signaling pathways activated and a significant number of inflammatory factors detectable in joint fluid and serum.<sup>5</sup> Cytokines such as tumor necrosis factor- $\alpha$  (TNF- $\alpha$ ) and interleukin-1 (IL-1) are particularly noteworthy. The accumulation of these inflammatory mediators is believed to disrupt intracellular homeostasis, leading to abnormal chondrocyte function. This dysfunction is manifested by the aberrant secretion of matrix metalloproteinases (MMPs), a class of zinc-dependent endopeptidases that play a crucial role in the metabolism and remodeling of cartilage tissues; however, during the pathology of OA, the abnormal expression and increased activity of MMPs are considered key factors in accelerating cartilage matrix degradation. This accelerated degradation not only alters the physical and chemical properties of cartilage tissues but may also further activate the inflammatory response, creating a vicious cycle that exacerbates OA progression. Moreover, B and T lymphocyte populations are altered in the context of inflammation and OA, with reduced regulatory functions. Identifying these potential pathogenic pathways may help pinpoint therapeutic targets for the treatment or prevention of OA.<sup>6,7</sup>

Currently available pharmacologic treatments for OA include oral and topical non-steroidal anti-inflammatory drugs (NSAIDs) and intra-articular corticosteroid injections. Non-pharmacologic modalities encompass biomechanical interventions, exercise management, strength training, and weight management.<sup>8,9</sup> Most of these treatments relieve the symptoms of OA but do not address the underlying cause of the disease, which is chronic inflammation. Although non-selective NSAIDs can suppress inflammation, they are known to cause gastrointestinal toxicity, such as dyspepsia, gastritis, and gastric ulcers.<sup>10</sup> In recent years, new therapeutic modalities have emerged in the treatment of OA, such as autologous chondrocyte implantation (ACI), matrix-induced autologous chondrocyte implantation (MACI), and arthroscopic debridement. However, these procedures often carry the risk of neurological or vascular injury and an immune response.<sup>11,12</sup> For patients with end-stage OA, total knee replacement is recommended; however, it is challenging to avoid the risks associated with infection, deep vein thrombosis, and long-term complications.<sup>13,14</sup> The quest for effective treatment options with fewer side effects is ongoing.

Curcumin, a phenolic extract derived from the rhizome of the ginger plant, is commonly used as a spice in food and is one of the most widely utilized natural agents. It boasts a wealth of biological activities, including anti-inflammatory, antioxidant, and anti-apoptotic properties. Curcumin regulates various molecular targets and signaling pathways, cell cycle proteins, cytokines, and chemokines. Curcumin has been widely used for centuries with a broad range of applications, leading to increased demand as a source of natural products for various medical and healthcare programs, such as those for cancer, endocrine-related disorders, cardiovascular-related diseases, and OA.<sup>15,16</sup> Zhang et al<sup>17</sup> used curcumin to treat a mouse model of destabilization of the medial meniscus (DMM) OA and found that it inhibited the expression of MMPs and suppressed synovitis and cartilage destruction, as demonstrated by immunohistochemistry and histology. In addition, studies have demonstrated curcumin's efficacy in reducing pain, improving physical function, and enhancing the quality of life in patients with OA through numerous clinical trials.<sup>18</sup> The molecular mechanisms of curcumin in the treatment of OA, however, require further exploration.

Network pharmacology is an innovative and effective approach to systematically uncovering the molecular mechanisms of drugs.<sup>19</sup> The molecular docking method is a powerful computational technique used to model,

dock, and analyze small molecular weight structures and related disease targets. This method enables the screening of pharmacodynamic material bases through computational simulations, calculations, and analyses, facilitating the rapid and efficient discovery of new bioactive lead compounds from databases.<sup>20</sup> Therefore, this study investigated the molecular mechanisms by which curcumin inhibits chondrocyte apoptosis in OA, employing network pharmacology, molecular docking, and experimental validation.

## Materials and Methods

### Screening of Potential Targets of Curcumin and OA Apoptosis and Establishment of a Protein–Protein Interaction (PPI) Network

Curcumin was searched in the PubChem database to obtain the “SMILES” format of curcumin, which was then entered into the Swiss Target Prediction database (<http://www.swisstargetprediction.ch/>). This database can infer related targets through the structure of active substances. In addition, curcumin was searched in the HERB database (<http://herb.ac.cn/>) to obtain curcumin-related targets. Furthermore, related curcumin targets were obtained from the DrugBank database (<https://www.drugbank.ca/>). The targets obtained from these methods were comprehensively summarized, and the target information was compared and verified using the UniProt database (<https://www.uniprot.org/>).

We searched the GeneCards database (<https://www.genecards.org/>) and the DisGeNET database ([www.disgenet.org/search](http://www.disgenet.org/search)) for “osteoarthritis” to identify OA-related targets. Chondrocyte-related targets were screened by searching “chondrocyte” in the GeneCards database. The common targets were imported into the STRING website, and the screening conditions were set to “*Homo sapiens*” species, with the lowest interaction score set to 0.4. The PPI network diagram was downloaded, and the results were imported into Cytoscape 3.9.0 to visualize the PPIs. Concurrently, the CytoNCA plug-in was used to perform topological analysis on the interaction network to obtain degree centrality. Based on the topology analysis results, potential targets were further screened from the active ingredient-disease intersection targets.<sup>21</sup>

### Biological Function and KEGG Pathway Analysis

To explore the role of curcumin’s potential target proteins in gene function and signaling pathways, we utilized the Metascape database (<https://metascape.org>) for annotation, visualization, and integration analysis. We analyzed the gene ontology (GO) of curcumin’s target proteins, including cellular components (CC), molecular functions (MF), and biological processes (BP), and selected those with p-values less than 0.01. The analysis results are presented as a bubble diagram, where the bubble size represents the number of enriched genes. Additionally, we used the Metascape database for KEGG pathway analysis to identify important signaling pathways that may be involved in the treatment of OA.

### Molecular Docking

To assess the reliability of curcumin-target interactions and explore the accurate binding mode, we selected the core gene as the molecular receptor and curcumin for molecular docking analysis. The original file of curcumin (MOL2 format) was downloaded from the PubChem database (<https://pubchem.ncbi.nlm.nih.gov/>), and the original file of the target protein was obtained from the RCSB PDB (<http://www.rcsb.org/>). Subsequently, we imported the protein structure into PyMOL version 2.4.1 (<https://pymol.org/2/>) and performed modifications, including the removal of water molecules, separation of ligands, and addition of hydrogen atoms. Molecular docking was performed using AutoDock Vina version 1.1.2. The binding energy of the molecule was analyzed, and the conformation with the lowest binding energy was selected. After observing the formation of hydrogen bonds, the structure was converted to PDBQT format for image modification in PyMOL.

### Reagents and Antibodies

Curcumin (458–37-7) and nitric oxide donor (SNP) were purchased from Spark Jade (Shandong, China). 0.25% trypsin, CCK-8 kit, cell counting reagent, 2,7-dichlorodihydrofluorescein diacetate (DCFH-DA) kit, Annexin V-Fluorescein isothiocyanate (FITC) /propidium iodide (PI) cell apoptosis staining kit, Hoechst 33342 staining kit, JC-1 mitochondrial

membrane potential detection kit, and calcein-AM/PI live/dead cell double staining kit were purchased from Bitian (Jiangsu, China). The C28 cell line, fetal bovine serum (FBS), DMEM/F12 medium, and Phosphate-Buffered Saline (PBS) were obtained from Zhongqiao Xinzhou (Shanghai, China). Enzyme-linked immunosorbent assay (ELISA) kits for IL-1, TNF- $\alpha$ , and IL-6, as well as antibodies against IL-6, COX-2, and MMP-1, and secondary antibodies, were purchased from Proteintech (Wuhan, China). Antibodies against Caspase-3, Bcl-2, PKC $\delta$ , MEKK3, ASK1, and GAPDH were purchased from Boster (Wuhan, China). Additionally, antibodies against p38, p-p38, Mmp-9, and p-PKC $\delta$  were purchased from Servicebio (Wuhan, China).

## Cell Culture

The medium in the original culture flask was removed, and the cells were washed twice with PBS. They were then digested with trypsin in 1–2 mL of 0.25% Ethylenediaminetetraacetic acid (EDTA) for 2 min. Digestion was monitored under a microscope. When the cell edges became rounded and detached from the adherent state, trypsin was removed, 6–8 mL of complete medium was added, and the cell layer was gently resuspended. A portion of the cell suspension was transferred to a new T-25 flask, and the appropriate complete medium was added. The cells were cultured in the incubator, with the medium being changed regularly. The process of passaging or cryopreserving was repeated when the cell density reached 70–80%.

## Chondrocyte Viability Analysis

The apoptosis model was established using SNP, and the toxicity of curcumin to cells was assessed. Chondrocytes ( $5 \times 10^3$  cells/cm<sup>2</sup>) were seeded and cultured in 96-well plates at 37°C for 24 h. The cells were incubated with SNP (0, 0.5, 1, and 2 mM) and curcumin (0, 5, 10, and 20  $\mu$ M). To quantitatively analyze cell viability at specific time points, we added 10  $\mu$ L of CCK-8 reagent to each well and incubated at 37°C for 2 h. The optical density (OD) was measured using an automatic microplate reader at a wavelength of 450 nm, with the OD value being proportional to cell viability. After determining the working concentrations of SNP and curcumin, we added 2 mM SNP to each well to treat cells for 24 h, followed by the addition of different concentrations of curcumin (0, 5, 10, and 20  $\mu$ M). Cell viability was then evaluated after 12, 24, and 48 h. For each well, 10  $\mu$ L of CCK-8 solution was added and incubated at 37°C for 2 h, after which the OD value at 450 nm was measured and analyzed using a microplate reader. A calcein-AM/PI live/dead cell double staining kit was employed to assess cell viability. Initially, the original supernatant was collected, and all cells were harvested after trypsin digestion. The collected cells were centrifuged at 800 g for 3–5 min, the supernatant was removed, and the cells were thoroughly washed with PBS 2–3 times. The calcein-AM/PI detection working solution was then added to resuspend the cells to a density of  $1 \times 10^6$  cells/mL. The cells were incubated in the dark for 15–30 min. Using a fluorescence microscope (FV31S-SW, Olympus, Japan), we observed and analyzed the levels of live and dead cells. Live cells labeled with calcein-AM exhibited green fluorescence, while dead cells labeled with PI exhibited red fluorescence.

## Detection of Intracellular Reactive Oxygen Species (ROS)

Intracellular ROS levels were measured using DCFH-DA. Chondrocytes ( $10 \times 10^4$  cells/cm<sup>2</sup>) were seeded in 24-well plates. The cells were treated as described above, the cell culture medium was removed, and an appropriate volume of diluted DCFH-DA (10  $\mu$ M) was added to completely cover the cells. Cells were incubated at 37°C for 20 min. The cells were then washed three times with serum-free cell culture medium to fully remove uninternalized DCFH-DA and unoxidized DCFH. Observed using a fluorescence microscope with an excitation wavelength of 490 nm and an emission wavelength of 520 nm.

## Detection of Mitochondrial Membrane Potential in Cells

Chondrocytes ( $10 \times 10^4$  cells/cm<sup>2</sup>) were seeded in 24-well plates and treated as described previously. After washing the cells with PBS, we added the JC-1 probe to each well and incubated in the dark at 25°C for 37 min and subsequently photographed using a fluorescence microscope.

## Apoptosis Analysis via Hoechst 33342 Staining

Hoechst 33342 staining was performed to detect the extent of apoptosis in chondrocytes. Chondrocytes ( $10 \times 10^4/\text{cm}^2$ ) were seeded in 24-well plates and treated as described previously. 1 mL of Hoechst 33342 dye was added to each well and incubated at 37°C for 15 min. The cells were then washed twice with PBS and photographed using a fluorescence microscope.

## Flow Cytometry Analysis

An annexin V-FITC/PI apoptosis staining kit was used to measure the degree of apoptosis in chondrocytes across different groups. After the cells were treated as described earlier, the chondrocytes in each group were washed with PBS and digested with trypsin without EDTA for 5 min. The cells were then collected by centrifugation at 1200 rpm for 5 min and suspended in 200  $\mu\text{L}$  of binding buffer. Subsequently, 4  $\mu\text{L}$  of annexin V-FITC and PI were added to the flow tube and incubated in the dark for 10 min. Cell apoptosis was analyzed using a BD FACS Aria II SORP flow cytometer (BD Biosciences, USA) at 488 nm.

## Western Blotting

To explore the effect of curcumin on SNP-induced chondrocyte apoptosis, we extracted total cellular proteins using a lysis buffer containing a protease inhibitor mixture. After Centrifuge at 12,000 rpm for 4 min, the supernatant from each group was collected. The protein concentration of the chondrocytes in each group was measured using a Bicinchoninic Acid (BCA) protein detection kit. Total cellular proteins (20  $\mu\text{g}$ ) from different groups were separated by SDS-polyacrylamide gel electrophoresis and electroporated onto polyvinylidene fluoride (PVDF) membranes. After blocking the membrane with 5% skim milk at room temperature for 90 min, we incubated the membranes with primary antibodies at 4°C overnight for western blotting analysis. The bands were then washed three times with Tris-buffered saline with Tween(TBST) and incubated with the secondary antibody at room temperature for 90 min. Afterward, the membrane was washed with TBST three times, and a chemical imaging system (Bio-Rad, USA) was employed to detect and analyze the density of each band.

## Immunofluorescence Staining

Chondrocytes were seeded into 24-well plates ( $2 \times 10^4$  cells per well). After various treatments, the cells were fixed with 4% paraformaldehyde for 15 min and permeabilized with 0.2% Triton X-100 (Servicebio, Wuhan, China) for 5 min. Subsequently, the cells were blocked with 5% bovine serum albumin (Servicebio, Wuhan, China) at room temperature for 1 h, incubated with the primary antibody at 4°C for at least 14–16 h, and then incubated with a fluorescent secondary antibody of the same species in the dark at room temperature for 1 h. Finally, the cells were stained with DAPI reagent for 10 min, excess dye was removed, the cells were washed, and fluorescence images were captured using a fluorescence microscope.

## Establishment of an Animal Model

We purchased 40 male Sprague–Dawley (S–D) rats (8 weeks old, weighing 300–350 g) from the Animal Center of the Medical College of Xi'an Jiaotong University (Xi'an, China). All animal experiments followed the National Institutes of Health Guidelines for the Care and Use of Laboratory Animals. Arthrotomy was performed on 10S–D rats without stripping the medial meniscus from their knee joints, which served as sham controls. OA was induced by medial meniscus stripping. The rats were randomly divided into four groups: a sham operation group, an OA group, a low-dose curcumin treatment group, and a high-dose curcumin treatment group. Immediately after surgery, curcumin was administered through gavage once daily for 12 weeks. We employed curcumin at low (50 mg/kg) and high (150 mg/kg) doses in our study. After 12 weeks of treatment, all rats were euthanized for subsequent testing.

## ELISA

At the 12th week of treatment, the rats were euthanized, and synovial fluid was collected. The concentrations of IL-1, IL-6, and TNF- $\alpha$  were measured using an ELISA kit.

## Micro-Computed Tomography (Micro-CT) Analysis

After fixing the knee with 4% paraformaldehyde overnight, we scanned the knee joint using a micro-CT system (SkyScan 1176, Bruker, Belgium). The scanning range included the cartilage and subchondral bone of the entire knee joint. Quantitative morphological measurements were determined from microscopic tomography data based on three-dimensional morphometry. Subsequently, the following indicators were evaluated: bone volume fraction (BV/TV), average trabecular thickness (Tb.Th), average trabecular number (Tb.N), and average trabecular spacing (Tb.Sp). These indicators indicate the quality and strength of the bone, which is crucial for evaluating the degree and therapeutic effect of OA.

## Histological Analysis

The right and left knee joints of different groups of rats were collected, and the cartilage tissues from each group were fixed in 4% paraformaldehyde for 24 h. The specimens were then decalcified with 10% EDTA for 1 month. Subsequently, cartilage from each group was dehydrated, embedded in paraffin, and cut into 5- $\mu$ m tissue sections. Safranin O (S-O) staining, hematoxylin and eosin (H&E) staining, and toluidine blue (TB) staining were performed to assess the degradation of the articular cartilage in each knee joint. Cartilage damage was assessed according to the Osteoarthritis Research Society International (OARSI) criteria, which involves scoring the depth and extent of damage, as well as bony encumbrances. This scoring system categorizes the damage into six grades, ranging from slight degeneration (0.5 points) to severe degradation (6 points). These scores are combined to form a total score reflecting the extent of damage to the entire articular cartilage.<sup>22</sup> Subsequently, the severity of OA lesions was quantified using a modified Mankin scoring system on a scale of 0 to 13. The Mankin scoring system consists of three components: structural abnormalities (0–6 points, with 0 representing normal and 6 representing complete structural disorganization), cellular abnormalities (0–3 points, with 0 representing normal and 3 representing cellular hypoplasia), and matrix staining (0–4 points, with 0 representing normal staining and 4 points representing the absence of stromal staining).<sup>23</sup> To minimize scoring bias, five professionally trained technicians conducted scoring independently under blinded conditions. This rigorous scoring procedure ensured the objectivity and accuracy of the scoring.

## Statistical Analysis

The experiments were conducted at least three times. Our results are expressed as the mean  $\pm$  standard deviation (SD). SPSS 23.0 software and GraphPad Prism 9.0 were used to analyze the data. One-way analysis of variance (ANOVA) was applied when the data satisfied the conditions of homogeneity of variance and normal distribution. The Kruskal–Wallis *H*-test was used to analyze non-parametric data (OARSI, Mankin score). A *p*-value of less than 0.05 was considered to indicate statistical significance.

## Results

### Enrichment Analysis and Molecular Docking of Curcumin with Chondrocytes

A total of 259 OA-related targets, 285 curcumin-related targets, and 375 chondrocyte-related targets were obtained. The curcumin targets were intersected with OA and chondrocyte-related targets, and a Venn diagram was drawn to identify the intersecting targets (Figure 1A). The 22 common genes obtained were uploaded to the STRING database to generate a PPI network. The results were then imported into Cytoscape 3.9.0 software for the analysis of the topological parameters of the network (Figure 1B). The results of the enrichment analysis are shown in Figure 1C and D. We selected the top five significant enrichment items of BPs, MFs, and CCs and found that the BPs primarily involved cellular responses to chemical stress, oxidative stress, among others. The KEGG analysis identified five main enrichment pathways. On the basis of the enrichment results and previous studies, we speculated that oxidative stress, apoptosis, and the p38 mitogen-activated protein kinase (p38/MAPK) signaling pathway play important roles in the progression of OA.<sup>24,25</sup> According to the aforementioned data, the core targets were separately imported into the AutoDock Vina 1.1.2 software and docked with curcumin (Figure 1E). Hydrogen bonds formed between the molecules are represented by yellow dotted lines in Figure 1E, and the relevant binding energies are shown in Table 1. Molecular docking simulations demonstrated that curcumin could interact well with these targets.

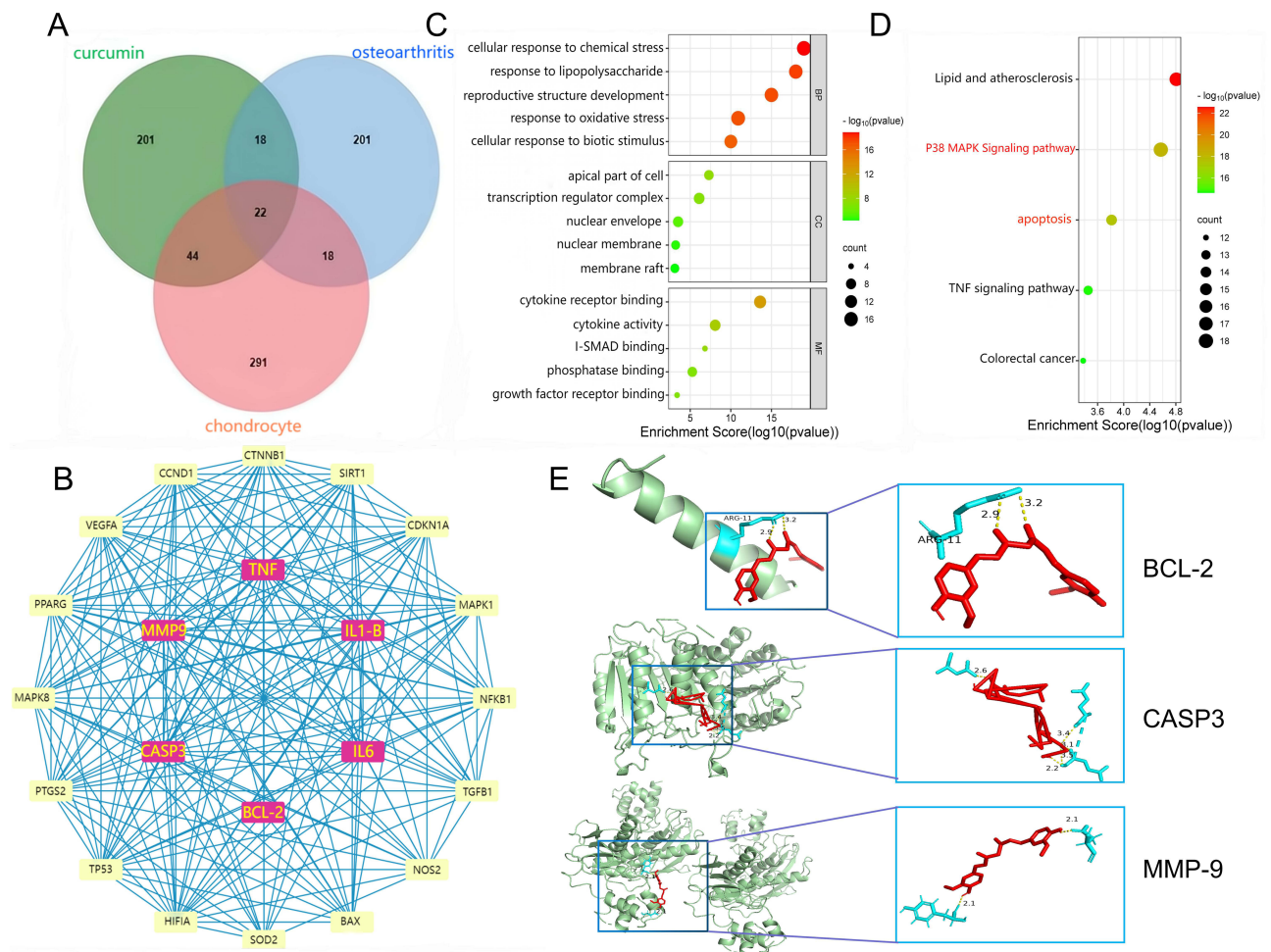


**Figure 1** Results of network pharmacology and molecular docking. **(A)** Curcumin and OA- and chondrocyte-related target distribution. Screened drugs may act on the core targets. **(B)** The interaction network of potential targets of curcumin in the treatment of osteoarthritis, wherein the top six targets of node degree are indicated with pink color. **(C and D)** BPs, CCs, MFs and KEGG analysis results, The size of the bubble represents the number of significantly different related targets enriched in the pathway, and the points with different color gradients represent the range of p values. The higher the enrichment factor value, the higher the enrichment degree, and the lower the p value, the higher the enrichment degree. **(E)** Curcumin was docked with Bcl-2, caspase-3, and Mmp-9, respectively. The red structure represents curcumin; the blue fragment on the protein structure represents the amino acid that forms hydrogen bonds with curcumin; and the yellow dotted line represents the hydrogen bond formed between the molecule and the protein.

## Effects of Curcumin on Chondrocyte Viability

To evaluate the impact of curcumin on the viability of chondrocytes treated with SNP, we employed the CCK-8 method to determine the effect of varying concentrations of curcumin on chondrocyte viability after 12, 24, and 48 h. We found that chondrocyte viability significantly decreased after treatment with 2 mM SNP ([Supplementary Figure 1A](#)), while curcumin exhibited no toxic effects on chondrocytes at concentrations  $\leq 10 \mu\text{M}$  ([Supplementary Figure 1B](#)). Given that

**Table 1** Docking Binding Energies and Number of Hydrogen Bonds of Curcumin with BCL-2, CASP3 and MMP-9

Molecule	Binding Energy (Kcal/mol)	Hydrogen Bond
Curcumin and CASP3	-6.48	6
Curcumin and MMP9	-5.45	2
Curcumin and BCL-2	-4.02	2

OA is a chronic degenerative disease associated with continuous oxidative stress, we selected 2 mM SNP as an in vitro stimulant to mimic OA-related oxidative stress, exposing rat chondrocytes to SNP for 24 h. We found that curcumin at a concentration of 5  $\mu$ M effectively inhibited the decline in chondrocyte viability induced by SNP (Figure 2A). Apoptosis of chondrocytes in different treatment groups was assessed through Hoechst 33342 staining and flow cytometry. The results indicated that SNP significantly increased the apoptosis rate of chondrocytes, indicating that SNP could induce chondrocyte apoptosis. Conversely, curcumin effectively reduced the apoptosis rate in chondrocytes, suggesting a protective effect against SNP-induced apoptosis (Figure 2B). Additionally, we employed a calcein AM/PI kit to detect the effect of curcumin on the chondrocyte death rate induced by SNP, with red staining indicating dead cells and green staining indicating normal cells. The results showed that curcumin at a concentration of 5  $\mu$ M significantly reduced the chondrocyte death rate (Figure 2C and D). On the basis of these results, we selected 5  $\mu$ M curcumin and 2 mM SNP as the optimal experimental conditions for subsequent experiments.

## Curcumin Inhibits SNP-Induced Oxidative Stress and Mitochondrial Dysfunction

Inflammation plays a significant role in the pathogenesis of OA. Inflammatory stimuli can lead to mitochondrial dysfunction, which in turn stimulates excessive production of ROS, creating a vicious cycle. To investigate the effect

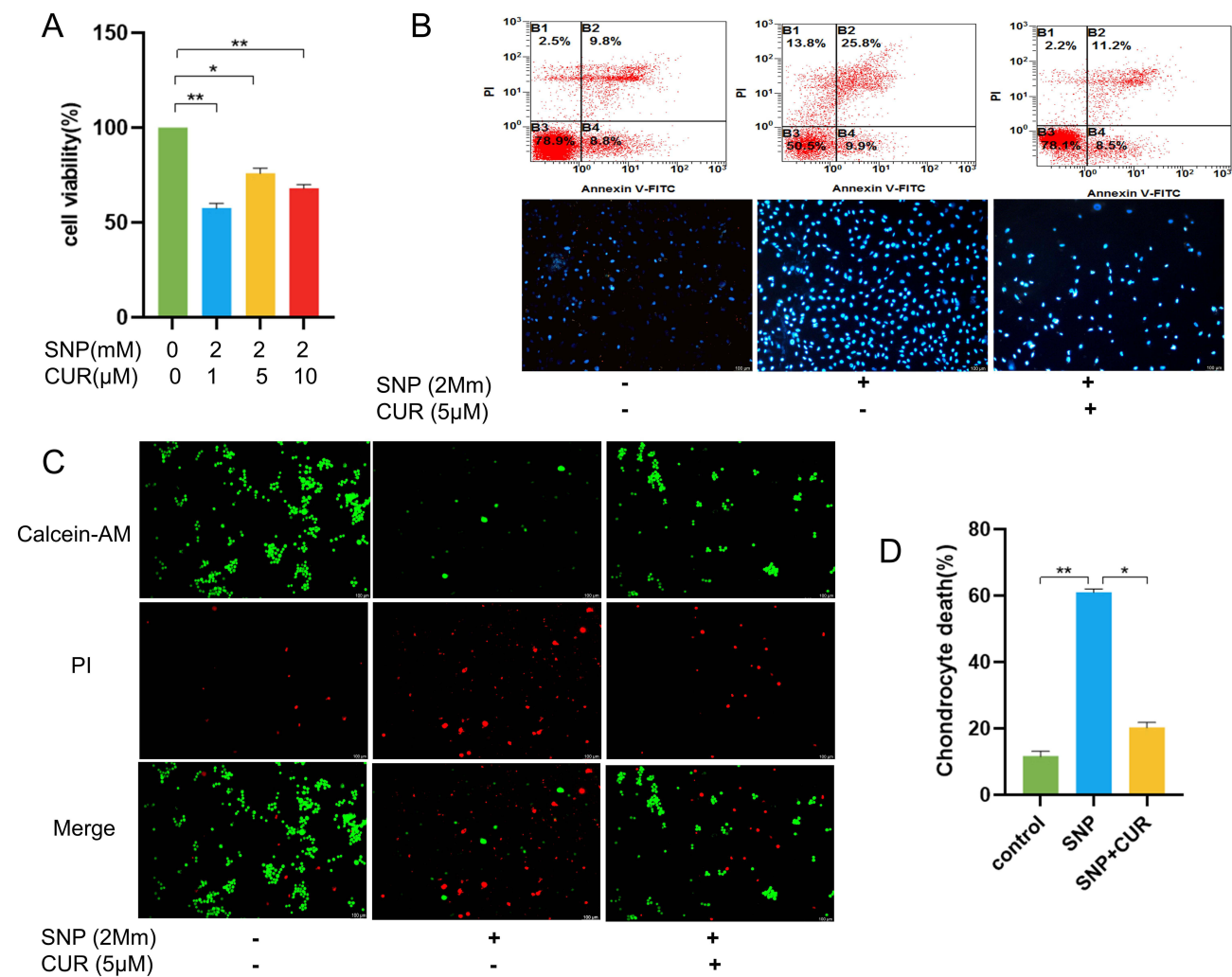


**Figure 2** Effect of curcumin on the viability of chondrocytes with or without curcumin. (A) Effects of varying concentrations of curcumin on chondrocytes stimulated by 2 mM SNP. (B) Hoechst 33342 fluorescence staining results (scale, 100  $\mu$ m) and flow cytometry apoptosis detection results. (C) The effect of curcumin on the viability of chondrocytes stimulated by 2 mM SNP (scale, 100  $\mu$ m). (D) Fluorescence quantitative analysis of the effects of curcumin on chondrocyte mortality stimulated by 2 mM SNP. (n = 3). \* $p$  < 0.05, \*\* $p$  < 0.01.



of curcumin on SNP-induced oxidative stress in chondrocytes, we employed the DCFH-DA fluorescent probe to measure ROS levels, where green fluorescence indicated ROS production. We found that chondrocytes in the control group exhibited almost no green fluorescence, whereas those in the SNP group displayed bright green fluorescence, indicating that SNP could significantly increase ROS production. However, chondrocytes in the curcumin-treated group showed weak green fluorescence, indicating that curcumin effectively inhibited ROS production (Figure 3A and B). To assess changes in mitochondrial function, we used the JC-1 fluorescent probe to detect variations in mitochondrial membrane potential. Green fluorescence indicates low mitochondrial membrane potential, while red fluorescence signifies high mitochondrial membrane potential. We found that the intensity of green fluorescence in chondrocytes in the SNP group was higher compared with that of red fluorescence, indicating that SNP significantly reduced mitochondrial membrane potential and led to mitochondrial dysfunction. In contrast, the curcumin group exhibited reduced green fluorescence intensity relative to red fluorescence, indicating that curcumin effectively increased mitochondrial membrane potential and improved mitochondrial function (Figure 3C and D). These results suggest that curcumin can protect OA chondrocytes by regulating SNP-induced oxidative stress and mitochondrial dysfunction.

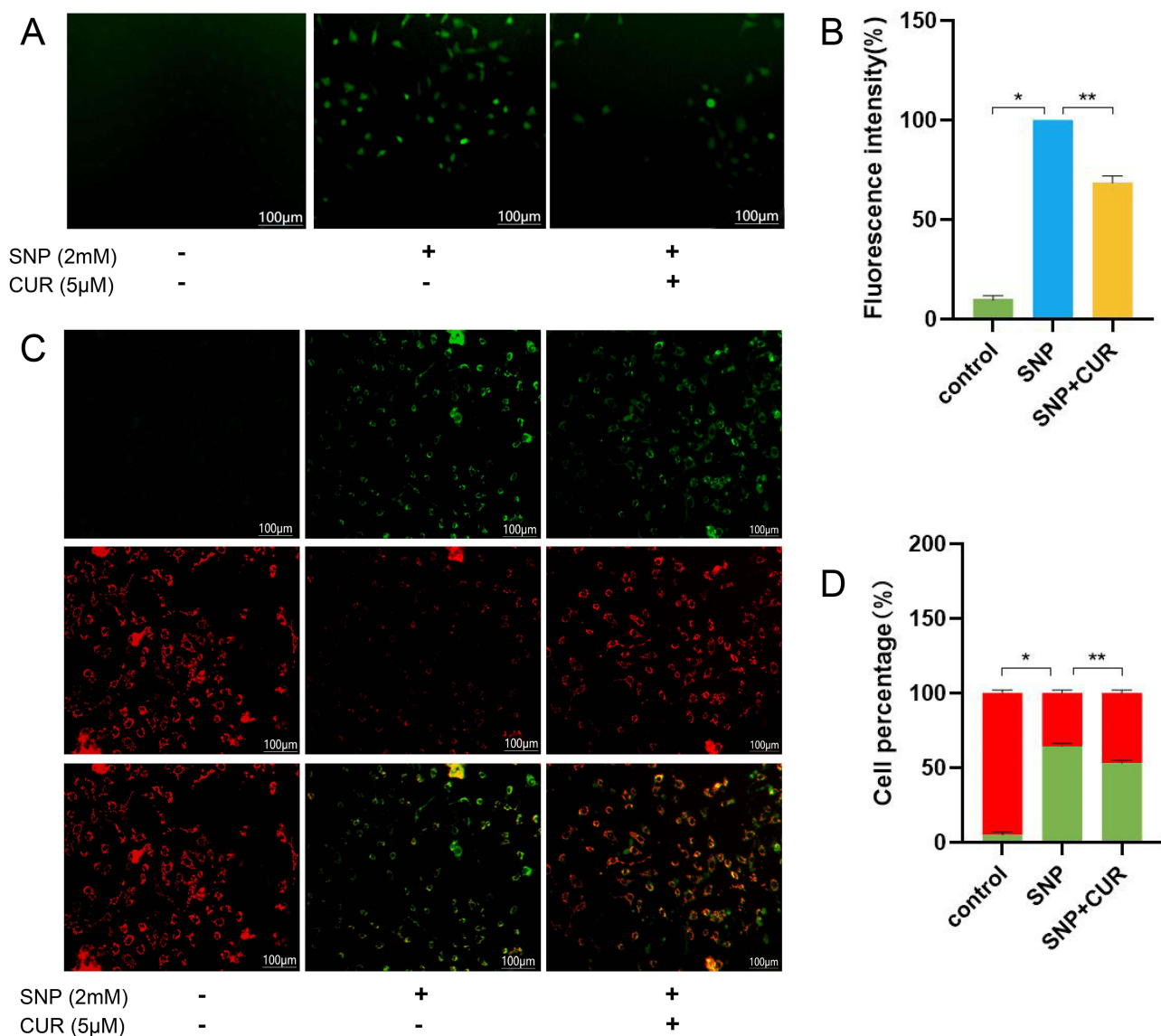


**Figure 3** Fluorescence analysis of oxidative stress and mitochondrial membrane potential. **(A)** Effect of curcumin on SNP-induced oxidative stress in chondrocytes (scale, 100 μm). **(B)** Fluorescence images of the quantitative analysis of ROS. **(C)** JC-1 emits red fluorescence in healthy mitochondria, while JC-1 green fluorescence indicates mitochondrial dysfunction. The combined images indicate co-localization (scale, 100 μm). **(D)** Fluorescence images of JC-1 quantitative analysis. (n = 3). \*p < 0.05, \*\*p < 0.01.

## Curcumin Inhibits SNP-Induced Inflammatory Response and Extracellular Matrix (ECM) Degradation

MMP-9 and MMP-1 are proteins capable of degrading major components of the ECM, such as type II collagen and proteoglycan. To determine whether curcumin can inhibit SNP-induced inflammatory response and cartilage ECM degradation, we treated chondrocytes with 2 mM SNP as an oxidative stress stimulator for 24 h, followed by the addition of 5  $\mu$ M curcumin to different groups for another 24 h. Immunofluorescence was used to detect the expression of MMP-9, MMP-1, and IL-6. The results showed that SNP significantly increased the expression levels of MMP-9, MMP-1, and IL-6, while curcumin effectively reversed this effect (Figure 4A–D). The original document is attached as [Supplementary Figure 2](#). To further validate these findings, we performed a Western blot to detect the expression levels of MMP-9, MMP-1, IL-6, and the inflammatory mediator COX-2. The results indicated that curcumin reduced the expression of MMP-9, MMP-1, IL-6, and COX-2 induced by SNP (Figure 4E–I). In summary, curcumin can inhibit the inflammatory response and ECM degradation in chondrocytes.

## Curcumin Inhibits SNP-Induced Chondrocyte Apoptosis by Regulating the p38/MAPK Signaling Pathway

To investigate the anti-apoptotic effect of curcumin on OA chondrocytes, we conducted Western blot analysis to assess the activity and phosphorylation status of p38 and MAPK. The results demonstrated a significant increase in p38 and

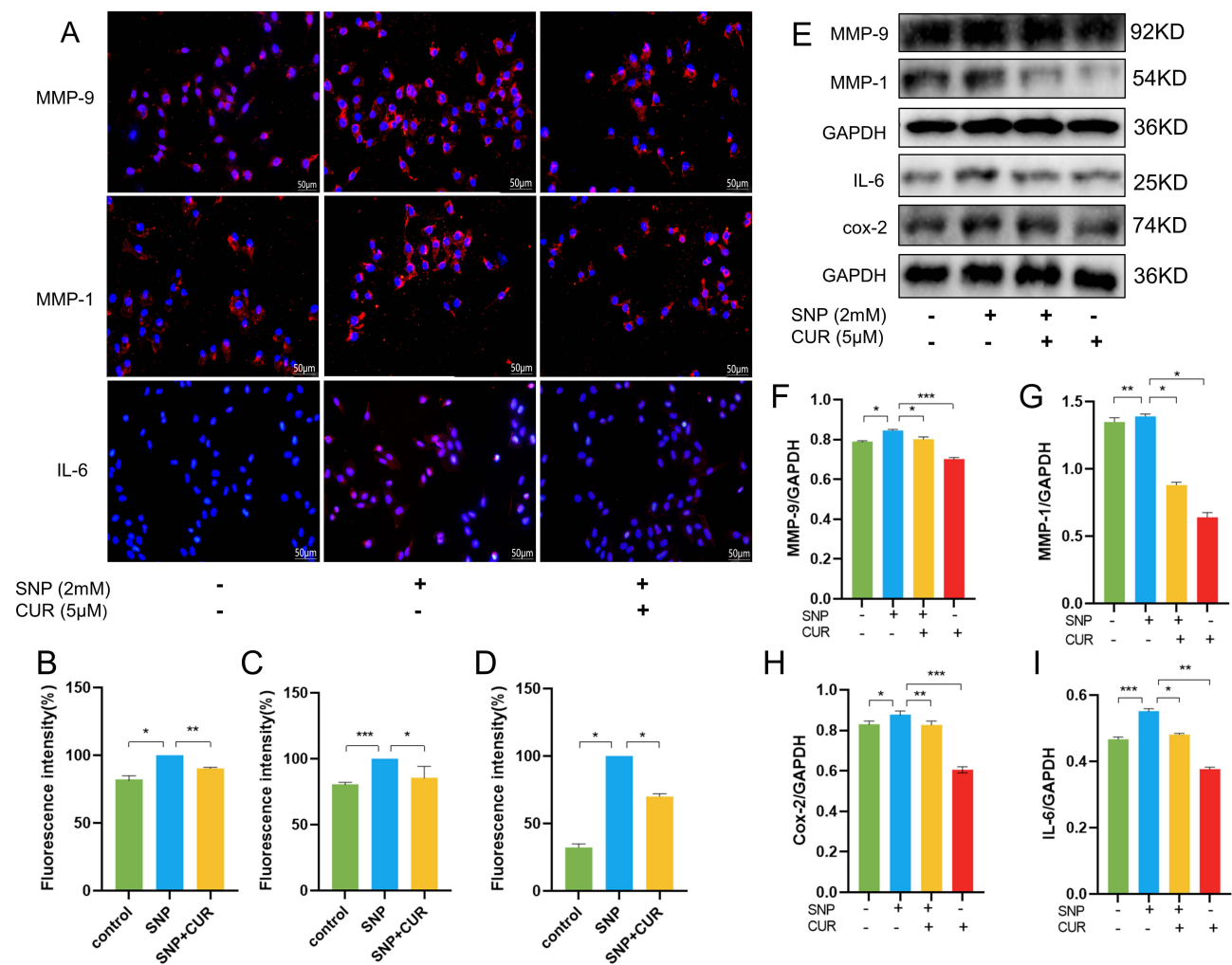


**Figure 4** Immunofluorescence and Western blot analysis of chondrocyte inflammation and matrix degradation. (A) Effects of curcumin on MMP-9, MMP-1, and IL-6 in SNP-induced chondrocytes (scale, 50  $\mu$ m). (B) MMP-9 fluorescence intensity quantitative analysis. (C) Quantitative analysis of MMP-1 fluorescence intensity. (D) IL-6 fluorescence intensity quantitative analysis. (E) Western blot images of MMP-9, MMP-1, IL-6, and COX-2. (F) MMP-9 Western blot quantitative analysis. (G) MMP-1 Western blot quantitative analysis. (H) COX-2 Western blot quantitative analysis. (I) IL-6 Western blot quantitative analysis. (n = 3). \* $p < 0.05$ , \*\* $p < 0.01$ , \*\*\* $p < 0.001$ .

MAPK phosphorylation upon SNP treatment, indicating activation of the p38/MAPK signaling pathway. Notably, curcumin effectively suppressed the phosphorylation of p38 and MAPK, suggesting its inhibitory role in modulating the activation of the p38/MAPK signaling pathway (Figure 5A–C).

To further investigate the mechanism of curcumin’s action, we assessed the expression levels of proteins involved in regulating the p38/MAPK signaling pathway. ASK1, an apoptotic signal-regulating kinase, can be activated by stress-related stimuli to activate MEKK4 and MEKK3, leading to p38 activation and the induction of apoptosis through signals associated with the mitochondrial cell death pathway.<sup>24,25,27</sup> We observed elevated levels of ASK1 and MEKK3 in the SNP group; however,

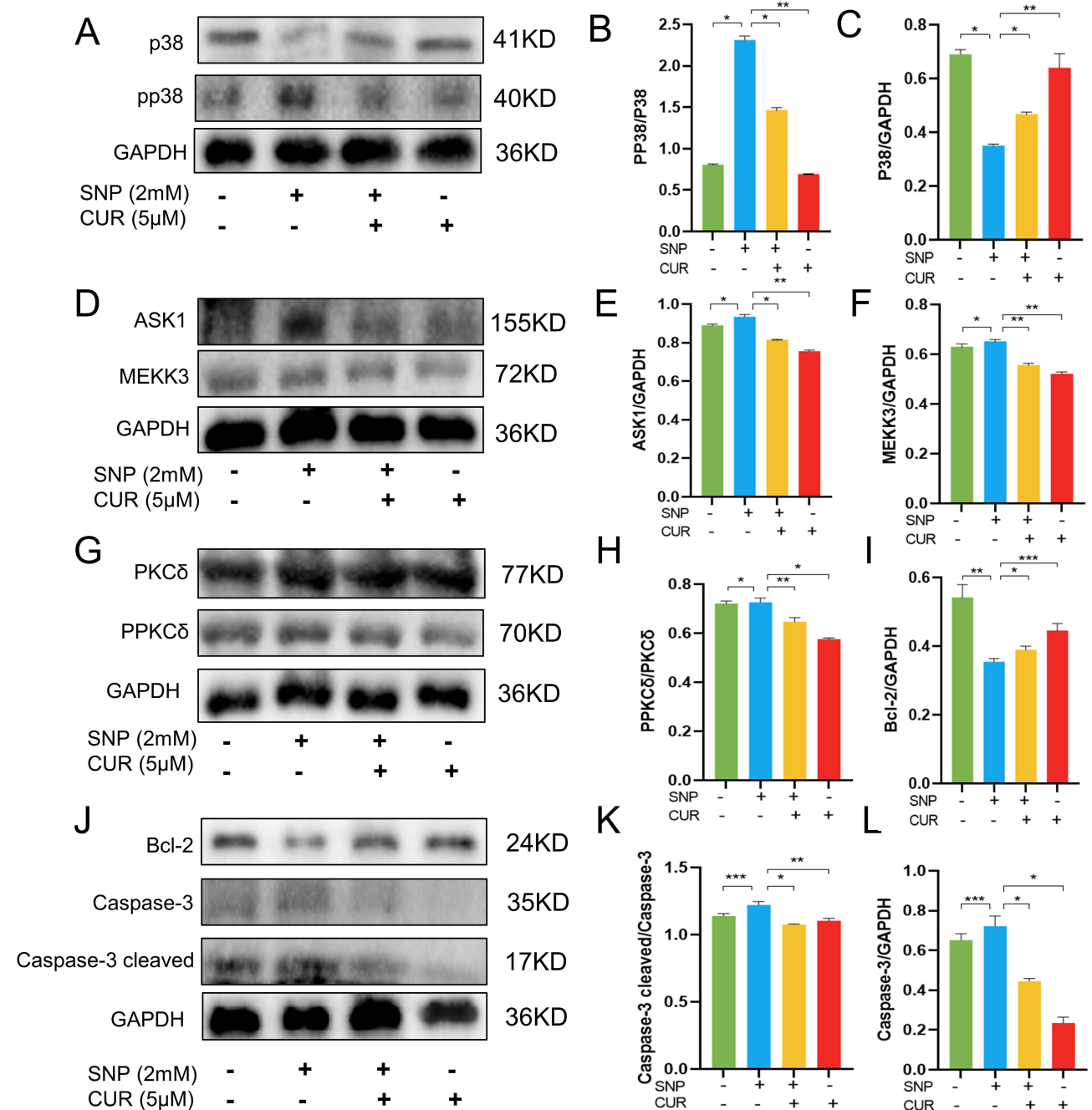


**Figure 5** Western blot analysis of curcumin regulation of the p38/MAPK pathway. (A–C) Western blot and quantitative analysis of p38 and p-p38. (D–F) Western blot and quantitative analysis of ASK1 and MEKK3. (G and H) Western blot images and quantitative analysis of PKCδ and p-PKCδ. (I–L) Western blot and quantitative analysis of BCL-2 and caspase-3. (n = 3). \*p < 0.05,\*\* p < 0.01,\*\*\*p < 0.001.

treatment with curcumin attenuated their expression (Figure 5D–F). Other studies have demonstrated that the inhibition of p38 phosphorylation can effectively suppress the activation of the p38/MAPK signaling pathway. Upon activation, p38 also activates ASK1 and MEKK3, thereby further stimulating p38/MAPK signaling.<sup>26</sup> Motivated by these findings, we proceeded to investigate the regulatory impact of curcumin on p38, revealing that curcumin exerted a significant influence on p38 phosphorylation (Figure 5G and H). Subsequently, we assessed the expression levels of the apoptosis-related proteins Bcl-2 and caspase-3. The results indicated that SNP significantly downregulated Bcl-2 expression while upregulating caspase-3 expression, suggesting its promotion of chondrocyte apoptosis. Notably, curcumin effectively inhibited chondrocyte apoptosis (Figure 5I–L).

In conclusion, these results suggest that curcumin can inhibit SNP-induced chondrocyte apoptosis by modulating the p38/MAPK signaling pathway, upregulating Bcl-2 expression, and downregulating caspase-3 expression. These actions collectively exert a protective effect on OA chondrocytes.

## Curcumin Attenuates Cartilage Degeneration and Osteophyte Formation

To evaluate the effect of curcumin treatment on cartilage degradation and osteoid formation in OA rats, we performed histological analyses employing H&E, SO, and TB staining (Figure 6A). H&E staining elucidated the morphological structure and cellular distribution of cartilage, SO staining revealed the proteoglycan content, and TB staining indicated the degree of bone mineralization and osteoid formation. H&E staining demonstrated that the cartilage in the sham-operated group exhibited a regular morphological structure, with chondrocytes arranged in a columnar shape, sufficient cartilage matrix, and a smooth cartilage surface. In contrast, the operated group showed obvious cartilage destruction and erosion, characterized by a reduced number of chondrocytes, disorganized arrangement, decreased cartilage matrix, and an uneven cartilage surface. Compared with the surgery group, the curcumin-treated group showed a certain degree of

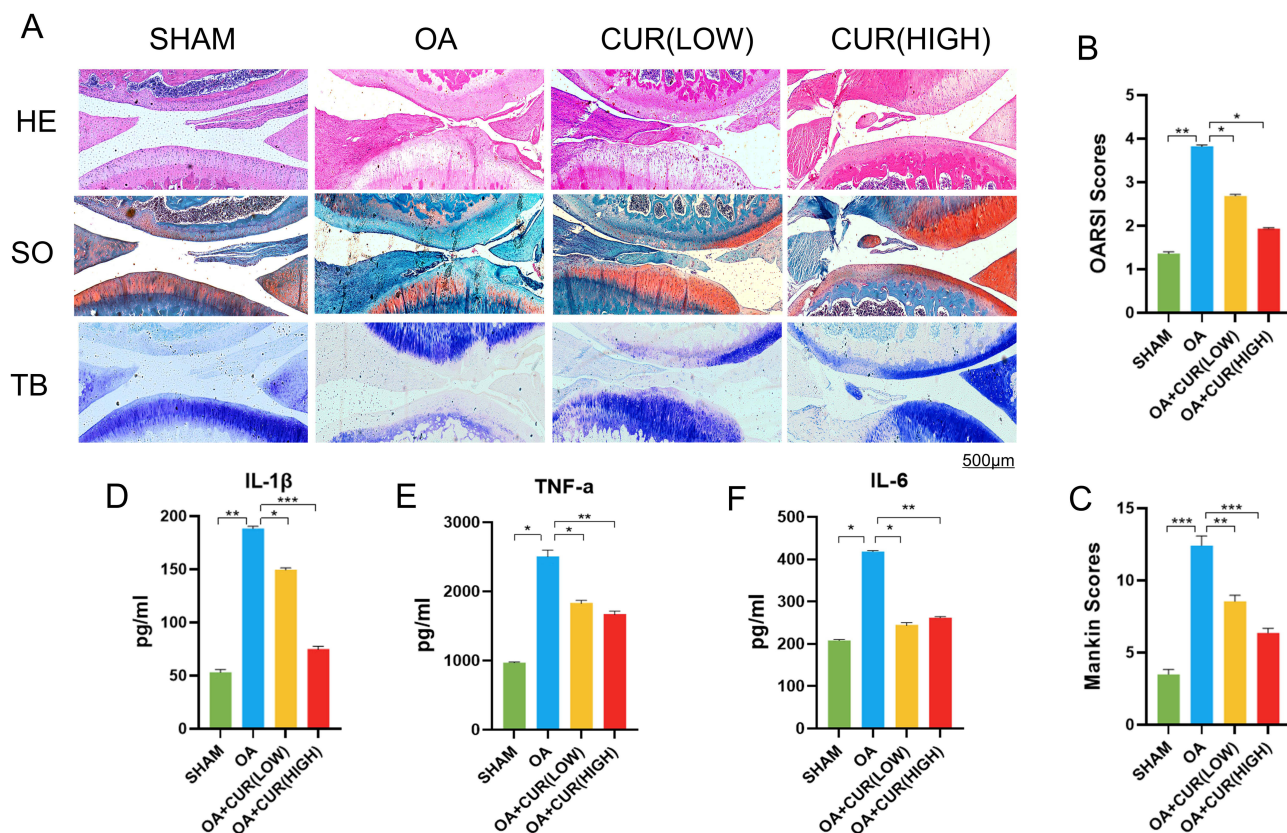


**Figure 6** Curcumin alleviated the progression of OA in a rat model. (A) Typical H&E, SO, and TB staining colors (scale, 500  $\mu$ m) of cartilage from various experimental groups (sham operation group, OA group, OA + curcumin (low) group, and OA + curcumin (high) group). (B) OARSI scores of the cartilage for the four groups. (C) Mankin scores of the cartilage for the four groups. (D–F) Rat articular fluid expression levels of IL-1, TNF- $\alpha$ , and IL-6. (n = 5). \* $p$  < 0.05, \*\* $p$  < 0.01, \*\*\* $p$  < 0.001.

cartilage repair, with an increased number of chondrocytes, a more regular arrangement, a more adequate cartilage matrix, and a flatter cartilage surface. SO staining showed that the cartilage in the sham-operated group appeared dark blue, indicating a high proteoglycan content and good elasticity and compression resistance in the cartilage. The cartilage in the surgery group displayed a light blue or colorless appearance compared to the sham-operated group, indicating low proteoglycan content and poor elasticity and compression resistance of the cartilage. In the curcumin-treated group, the cartilage appeared darker blue compared to the surgical group, indicating restored proteoglycan content and improved elasticity and compression resistance of the cartilage. TB staining revealed that bones in the sham-operated group were dark blue, indicating a high degree of mineralization and good hardness and strength of the bone. Compared to the sham-operated group, the bones in the operated group exhibited light blue or no color, indicating a low degree of bone mineralization and poor bone hardness and strength, along with visible bone recession, indicating hyperplasia and deformity of the bones. The bones in the curcumin-treated group were darker blue compared to the surgical group, indicating restored mineralization and improved bone hardness and strength. Additionally, fewer bony remnants were observed in the curcumin-treated group, indicating reduced bone proliferation and deformation.

To quantitatively assess the extent of cartilage damage, we employed the OARSI scale, which evaluates structural, cellular, matrix, and surface changes in cartilage. Higher scores on this scale indicate more severe cartilage damage. Our results revealed that the OARSI score was significantly higher in the surgery group compared to the sham surgery group. Conversely, the OARSI score was significantly lower in the curcumin-treated group than in the surgery group, suggesting that curcumin treatment reduced cartilage damage (Figure 6B). To further validate the therapeutic effect of curcumin, we quantified the severity of OA lesions using a modified Mankin scoring system, which ranges from 0 to 13. Compared with the sham-operated group, the Mankin score was significantly higher in the operated group of rats and significantly lower in the curcumin-treated group (Figure 6C). In summary, these results suggest that curcumin treatment significantly increases cartilage thickness, improves cartilage morphology, structure, and function, and decreases the OARSI score in OA rats. Additionally, curcumin attenuates bone mineralization disorders and the formation of osteochondroses, thereby playing a protective role for cartilage and bone in OA rats.

## Curcumin Inhibits Synovial Inflammation Factors in a Surgery-Induced OA Model

To explore the protective effect of curcumin on OA in rats, we established an OA model using S–D rats by cutting the anterior cruciate ligament. We then administered different doses of curcumin (50 or 100 mg/kg) via gavage, once a day, for 12 weeks. At the end of the experiment, we collected the synovial fluid of the rats and measured the levels of the inflammatory cytokines IL-1 $\beta$ , IL-6, and TNF- $\alpha$  through ELISA. These cytokines represent some of the cytokines that mediate inflammatory responses and play a crucial role in the pathogenesis of OA by stimulating chondrocytes to release MMPs and oxidative stress substances, leading to cartilage degradation. Our results showed that, compared with those in the sham group, the levels of IL-1 $\beta$ , IL-6, and TNF- $\alpha$  in the synovial fluid of the surgery group were significantly increased, indicating that surgery induced an inflammatory response in OA rats. Conversely, compared with those in the surgery group, the levels of IL-1 $\beta$ , IL-6, and TNF- $\alpha$  in the synovial fluid of the curcumin treatment group were significantly reduced, indicating that curcumin inhibited the inflammatory response in OA rats (Figure 6D–F).

## Curcumin Improves Subchondral Bone Resorption

To investigate the effects of curcumin on the structural changes in bone in OA rats, we utilized micro-CT for three-dimensional imaging and conducted quantitative morphological measurements. These measurements included BV/TV, trabecular thickness (Tb.Th), trabecular number (Tb.N), and trabecular separation (Tb.Sp). These indicators reflect bone density, strength, and continuity, which are associated with the degree of bone loss and remodeling. The results showed that surgical injury induced significant osteophyte formation and bone resorption, indicating that OA development led to bone hyperplasia and destruction. Curcumin treatment significantly increased BV/TV, Tb.Th, and Tb.N, and decreased Tb.Sp in OA rats, indicating that curcumin treatment improved bone density, strength, and continuity in these rats (Figure 7A–D). To quantitatively evaluate the structural changes in bone, we used ANOVA and Tukey's test to compare the differences between groups. The results showed that, compared with the sham operation group, the operation group exhibited significantly decreased BV/TV, Tb.Th, and Tb.N, along with a significantly increased Tb.Sp. Conversely,

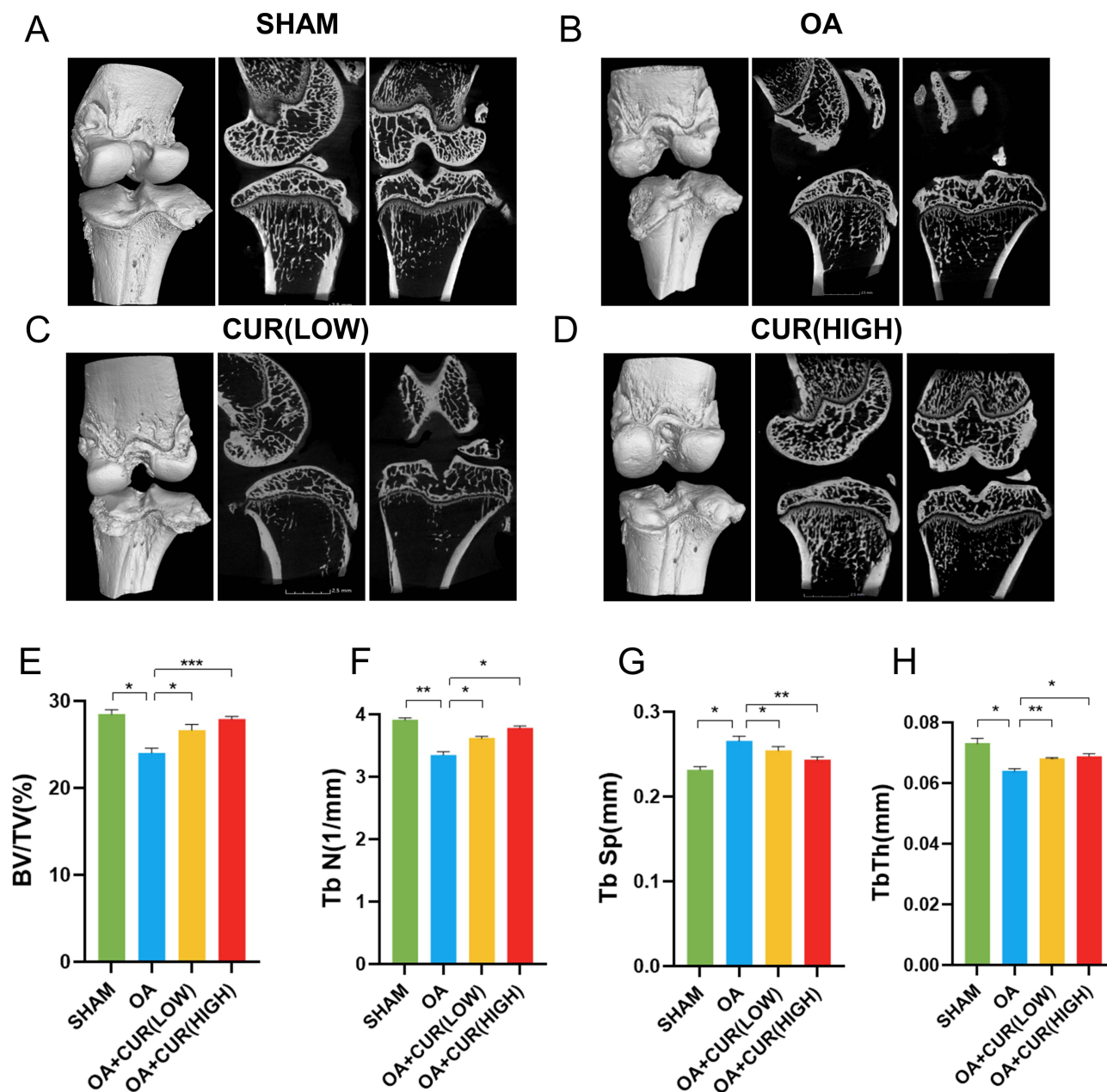


**Figure 7** Detection and quantitative analysis of micro-CT in the knee joints of different groups of rats. (A–D) The three-dimensional reconstruction of the knee joint in each group, as well as the sagittal and coronal planes. (E–H) Quantitative analysis of BV/TV, Tb.N, Tb.Sp, and Tb.Th. (n = 5). \* $p < 0.05$ , \*\* $p < 0.01$ , \*\*\* $p < 0.001$ .

compared with the operation group, the curcumin-treated group exhibited significantly increased BV/TV, Tb.Th, and Tb.N and significantly decreased Tb.Sp (Figure 7E–H). These results suggest that curcumin treatment can inhibit structural changes in the bones of OA rats, thereby protecting their bones.

## Discussion

OA is a common degenerative joint disease characterized primarily by the degeneration of articular cartilage and the apoptosis of chondrocytes.<sup>28</sup> Oxidative stress is a significant factor contributing to chondrocyte apoptosis, activating multiple inflammatory pathways, such as IL-1 $\beta$ , TNF- $\alpha$ , Lipopolysaccharides (LPS), and NO.<sup>5</sup> NO is a small molecule signaling substance with various physiological and pathological functions and plays a crucial regulatory role in chondrocytes. The level of NO in OA cartilage has been found to be positively correlated with the degree of chondrocyte

apoptosis, suggesting that NO plays a key role in the pathogenesis of OA.<sup>29</sup> Since articular cartilage lacks blood vessels, lymphatics, and nerve fibers, chondrocytes are the only cell type responsible for synthesizing and maintaining the ECM.<sup>30</sup> Apoptosis of chondrocytes leads to the long-term accumulation of apoptotic bodies in cartilage, which interferes with the metabolism of the ECM and ultimately damages the entire cartilage.<sup>31</sup> Buhrmann et al<sup>32</sup> established a pathological model of OA through in vitro experiments and found that curcumin regulates the homeostasis of the ECM by inhibiting the activation of NF- $\kappa$ B, thereby inhibiting chondrocyte apoptosis. In addition, Koboziev et al<sup>33</sup> validated the protective effect of curcumin on chondrocytes in a high-fat diet-induced obesity model in mice. Their findings support the findings of Buhrmann et al and further validate the protective effect of curcumin on chondrocytes in an in vivo model. Therefore, modulation of chondrocyte apoptosis is an important strategy for treating OA.

Curcumin can regulate cell survival and apoptosis through various signaling pathways, including the p38/MAPK pathway. The p38/MAPK pathway plays a broad range of physiological and pathological roles, such as in cellular oxidative stress, inflammatory responses, cell cycle regulation, apoptosis, differentiation, and migration.<sup>34</sup> The p38/MAPK pathway plays a vital role in the immune system, contributing to the secretion of inflammatory factors, antigen presentation, cytokine expression, cell activation, and proliferation. It also plays a significant role in the regulation of apoptosis, promoting or inhibiting cell death by influencing the expression and activity of apoptotic factors, such as Bcl-2, Bax, Bad, and caspase.<sup>33</sup> To the best of our knowledge, this is the first instance where network pharmacology combined with experiments has been used to determine the crucial role of the p38/MAPK signaling pathway in the curcumin treatment of OA. In OA, the activation of the p38/MAPK pathway is considered a key factor leading to chondrocyte apoptosis and ECM degradation.<sup>35</sup> Our study elucidated that curcumin could protect chondrocytes from OA by inhibiting the phosphorylation of p38/MAPK, thereby inhibiting the expression or activity of its downstream effectors, such as caspase-3, MMP-9, and Bcl-2. The inhibitory effect of curcumin on the p38/MAPK pathway may be attributed to its antioxidant properties, as oxidative stress is a significant stimulus for activating the p38/MAPK pathway.<sup>34</sup> In this study, we examined the expression levels of ROS in chondrocytes and found that curcumin significantly scavenges intracellular ROS, thereby effectively alleviating cellular damage induced by oxidative stress. Similarly, Chen et al<sup>36</sup> used curcumin to intervene in a chondrocyte inflammation model and reached consistent conclusions, validating curcumin's potential role in reducing oxidative stress. In addition, previous studies have revealed the regulatory effects of curcumin on chondrocyte apoptosis through various signaling pathways, including nuclear NF- $\kappa$ B, JNK, ERK, and PI3K/Akt. These findings highlight the multi-targeted mechanism of action of curcumin in regulating apoptosis.<sup>37,38</sup> All these signaling pathways interact with the p38/MAPK pathway, forming a complex signaling network that collectively determines cell fate.

Synovial inflammation is a chronic inflammatory response involving various cell types, such as synoviocytes, macrophages, T-cells, B-cells, and neutrophils.<sup>39</sup> These cells secrete numerous inflammatory factors, such as TNF- $\alpha$ , IL-1 $\beta$ , IL-6, IL-8, and IL-17, which can lead to chondrocyte apoptosis and cartilage matrix degradation.<sup>40</sup> Previous studies have shown that in a rat model of OA, curcumin treatment reduces the levels of NF- $\kappa$ B and its associated inflammatory factors, particularly by inhibiting the expression of TNF- $\alpha$  and IL-1 $\beta$ , which in turn exerts a protective effect on chondrocytes.<sup>41</sup> Similarly, we found that curcumin significantly inhibits the expression of TNF- $\alpha$ , IL-1, and IL-6, as revealed by ELISA. These inflammatory factors can also induce angiogenesis and increase blood vessel permeability, leading to the accumulation of immune cells in the synovial membrane and the formation of synovial granulation tissue, which can erode cartilage and bone, aggravating OA lesions.<sup>42</sup> Moreover, the accumulation of inflammatory factors increases osteoclast activity in arthritis, disrupting the balance between bone formation and bone resorption, ultimately leading to a significant reduction in subchondral bone thickness and further exacerbating OA.<sup>43</sup> Our micro-CT scans showed that curcumin increased the BV/TV of trabecular bone, increased the number of trabecular bones and decreased trabecular bone separation. Thus, curcumin slows the progression of OA by attenuating the loss of subchondral bone and improving bone microarchitecture. In summary, our study provides novel insights into the molecular mechanisms and targets for curcumin in the treatment of OA and provides novel avenues for developing OA drugs. As a natural, safe, and effective drug, curcumin is a promising new option for patients with OA.

## Conclusion

We found that curcumin modulates chondrocyte oxidative stress, inhibits OA inflammation, and inhibits phosphorylation of the p38/MAPK pathway. It also inhibits chondrocyte apoptosis and matrix degradation while promoting cartilage repair through multiple pathways and targets, as validated by network pharmacology, molecular docking techniques, and experimental studies. We elucidated the molecular mechanism of curcumin in OA treatment, providing valuable insights for its clinical application; however, the clinical application of curcumin is limited by its low bioavailability, primarily due to poor solubility, stability, and biobarrier permeability. Therefore, future studies should focus on improving the drug properties of curcumin. Strategies such as nanotechnology, liposome encapsulation, or combination with other drugs could enhance its bioavailability. In addition, to comprehensively assess the therapeutic efficacy of curcumin in OA, more animal models and ultimately clinical trials should be conducted to validate its safety and efficacy and to determine the optimal dosage, route of administration, and treatment duration.

## Institutional Review Board Statement

All animal experiments followed the National Institutes of Health Guidelines for the Care and Use of Laboratory Animals, Experiments involving animals have been approved by the Animal Ethics Committee of Xi'an Jiaotong University.(XJTUAE2023-1639). The public data information used in this study conforms to the ethical code of Xi'an Honghui Hospital(202406012).

## Data Sharing Statement

The data presented in this study are available in the article.

## Author Contributions

All authors made a significant contribution to the work reported, whether that is in the conception, study design, execution, acquisition of data, analysis and interpretation, or in all these areas; took part in drafting, revising or critically reviewing the article; gave final approval of the version to be published; have agreed on the journal to which the article has been submitted; and agree to be accountable for all aspects of the work.

## Funding

This work was supported by the Shaanxi Province Key Research and Development Plan (2020SF-099), Shaanxi Province Innovation Capability Support Plan (2021TD-59), Shaanxi Province Key Research and Development General Project-Social Development Field (2023-YBSF-488) and Xi'an Municipal Health Commission Cultivation Project (2023ms15).

## Disclosure

The authors declare that there is no conflict of interest.

## References

1. Johnson VL, Hunter DJ. The epidemiology of osteoarthritis. *Best Pract Res Clin Rheumatol*. 2014;28(1):5–15. doi:10.1016/j.berh.2014.01.004
2. Palazzo C, Nguyen C, Lefevre-Colau MM, et al. Risk factors and burden of osteoarthritis. *Ann Phys Rehabil Med*. 2016;59(3):134–138. doi:10.1016/j.rehab.2016.01.006
3. Sharma L, Kapoor D, Issa S. The epidemiology of osteoarthritis. *Curr Opin Rheumatol*. 2006;18(2):147–156. doi:10.1097/01.bor.0000209426.84775.f8
4. Abramoff B, Caldera FE. Osteoarthritis: pathology, diagnosis, and treatment options. *Med Clin North Am*. 2020;104(2):293–311. doi:10.1016/j.mcna.2019.10.009
5. Xia B, Chen D, Zhang J, et al. Osteoarthritis pathogenesis: a review of molecular mechanisms. *Calcif Tissue Int*. 2014;95(6):495–505. doi:10.1007/s00223-014-9917-9
6. Motta F, Barone E, Sica A, et al. Inflammaging and Osteoarthritis. *Clin Rev Allergy Immunol*. 2023;64(2):222–238. doi:10.1007/s12016-022-08835-0
7. Hodgkinson T, Kelly DC, Curtin CM, et al. Mechanosignalling in cartilage: an emerging target for the treatment of osteoarthritis. *Nat Rev Rheumatol*. 2022;18(1):67–84. doi:10.1038/s41584-021-00671-2
8. Kon E, Filardo G, Drobnic M, et al. Non-surgical management of early knee osteoarthritis. *Knee Surg Sports Traumatol Arthrosc*. 2012;20(3):436–449. doi:10.1007/s00167-011-1713-8



9. Alghamdi MA, Olney SJ, Costigan PA. Exercise treatment for osteoarthritis disability. *Ann Saudi Med.* 2004;24(5):326–331. doi:10.5144/0256-4947.2004.326
10. Rannou F, Pelletier JP, Martel-Pelletier J, et al. Efficacy and safety of topical NSAIDs in the management of osteoarthritis: evidence from real-life setting trials and surveys. *Semin Arthritis Rheum.* 2016;45(4 Suppl):S18–S21. doi:10.1016/j.semarthrit.2015.11.007
11. Sherman SL, Thyssen E, Nuelle CW. Osteochondral autologous transplantation. *Clin Sports Med.* 2017;36(3):489–500. doi:10.1016/j.csm.2017.02.006
12. Frehner F, Benthien JP. Microfracture: state of the art in cartilage surgery? *Cartilage.* 2018;9(4):339–345. doi:10.1177/1947603517700956
13. Liddle AD, Pegg EC, Pandit H. Knee replacement for osteoarthritis. *Maturitas.* 2013;75(2):131–136. doi:10.1016/j.maturitas.2013.02.014
14. Kamaruzaman H, Kinghorn P, Oppong R, et al. Cost-effectiveness of surgical interventions for the management of osteoarthritis: a systematic review of the literature. *BMC Musculoskelet Disord.* 2017;18(1):183. doi:10.1186/s12891-017-1525-3
15. Paultre KY, Cade W, Hernandez D, et al. Therapeutic effects of turmeric or curcumin extract on pain and function for individuals with knee osteoarthritis: a systematic review. *BMJ Open Sport Exerc Med.* 2021;7(1):e000935. doi:10.1136/bmjsem-2020-000935
16. Daily JW, Yang M, Park S. Efficacy of turmeric extracts and curcumin for alleviating the symptoms of joint arthritis: a systematic review and meta-analysis of randomized clinical trials. *J Med Food.* 2016;19(8):717–729. doi:10.1089/jmf.2016.3705
17. Zhang Z, Leong DJ, Xu L, et al. Curcumin slows osteoarthritis progression and relieves osteoarthritis-associated pain symptoms in a post-traumatic osteoarthritis mouse model. *Arthritis Res Ther.* 2016;18(1):128. doi:10.1186/s13075-016-1025-y
18. Chin KY. The spice for joint inflammation: anti-inflammatory role of curcumin in treating osteoarthritis. *Drug Des Devel Ther.* 2016;10:3029–3042. doi:10.2147/DDDT.S117432
19. Nogales C, Mamdouh ZM, List M, et al. Network pharmacology: curing causal mechanisms instead of treating symptoms. *Trends Pharmacol Sci.* 2022;43(2):136–150. doi:10.1016/j.tips.2021.11.006
20. Pinzi L, Rastelli G. Molecular docking: shifting paradigms in drug discovery. *Int J Mol Sci.* 2019;20(17):4331. doi:10.3390/ijms20174331
21. Batool K, Niazi MA. Towards a methodology for validation of centrality measures in complex networks. *PLoS One.* 2014;9(3):e90283. doi:10.1371/journal.pone.0090283
22. Liew JW, King LK, Mahmoudian A, et al. A scoping review of how early-stage knee osteoarthritis has been defined. *Osteoarthr Cartil.* 2023;31(9):1234–1241. doi:10.1016/j.joca.2023.04.015
23. Kumar S, Sugihara F, Suzuki K, et al. A double-blind, placebo-controlled, randomised, clinical study on the effectiveness of collagen peptide on osteoarthritis. *J Sci Food Agric.* 2015;95:702–707. doi:10.1002/jsfa.6752
24. Selimovic D, Kharouf N, Carrouel F, et al. Induction of antimicrobial protein S100A15 expression by oral microbial pathogens is toll-like receptors-dependent activation of c-Jun-N-Terminal Kinase (JNK), p38, and NF-κB Pathways. *Int J Mol Sci.* 2023;24(10):5348. doi:10.3390/ijms24105348
25. Hu Y, Lin L, Liu K, et al. L-Theanine alleviates heat stress-induced impairment of immune function by regulating the p38 MAPK signalling pathway in mice. *Food Funct.* 2023;14(1):335–343. doi:10.1039/D2FO02300A
26. Lu J, Yu M, Li J. PKC-δ promotes IL-1β-induced apoptosis of rat chondrocytes and via activating JNK and P38 MAPK pathways. *Cartilage.* 2023. doi:10.1177/19476035231181446
27. Hwang HS, Kim HA. Chondrocyte apoptosis in the pathogenesis of osteoarthritis. *Int J Mol Sci.* 2015;16(11):26035–26054. doi:10.3390/ijms161125943
28. Beltrán B, Mathur A, Duchon MR, et al. The effect of nitric oxide on cell respiration: a key to understanding its role in cell survival or death. *Proc Natl Acad Sci U S A.* 2000;97(26):14602–14607. doi:10.1073/pnas.97.26.14602
29. Aigner T, Kim HA, Roach HI. Apoptosis in osteoarthritis. *Rheum Dis Clin North Am.* 2004;30(3):639. doi:10.1016/j.rdc.2004.04.012
30. Wu L, Liu Z. The molecular mechanisms of preventing apoptosis of cartilage chondrocyte to target osteoarthritis. *Future Med Chem.* 2017;9(5):537–540. doi:10.4155/fmc-2016-0230
31. Xia L, Luo QL, Lin HD, et al. The effect of different treatment time of millimeter wave on chondrocyte apoptosis, caspase-3, caspase-8, and MMP-13 expression in rabbit surgically induced model of knee osteoarthritis. *Rheumatol Int.* 2012;32(11):2847–2856. doi:10.1007/s00296-011-2089-4
32. Buhmann C, Brockmueller A, Mueller AL, et al. Curcumin attenuates environment-derived osteoarthritis by Sox9/NF-κB signaling axis. *Int J Mol Sci.* 2021;22(14):7645. doi:10.3390/ijms22147645
33. Koboziev I, Scoggin S, Gong X, et al. Effects of curcumin in a mouse model of very high fat diet-induced obesity. *Biomolecules.* 2020;10(10):1368. doi:10.3390/biom10101368
34. Wei J, You G, Cheng H, et al. SPRED2 promotes autophagy and attenuates inflammatory response in IL-1β induced osteoarthritis chondrocytes via regulating the p38 MAPK signaling pathway. *Tissue Cell.* 2023;82:102086. doi:10.1016/j.tice.2021.102086
35. Cao X, Cai L, Guo D, et al. Fibroblast growth factor 8 facilitates cell-cell communication in chondrocytes via p38-MAPK signaling. *Tissue Cell.* 2023;83:102155. doi:10.1016/j.tice.2023.102155
36. Chen B, He Q, Chen C, et al. Combination of curcumin and catalase protects against chondrocyte injury and knee osteoarthritis progression by suppressing oxidative stress. *Biomed Pharmacother.* 2023;168:115751. doi:10.1016/j.biopha.2023.115751
37. Qiu B, Xu X, Yi P, et al. Curcumin reinforces MSC-derived exosomes in attenuating osteoarthritis via modulating the miR-124/NF-κB and miR-143/ROCK1/TLR9 signalling pathways. *J Cell Mol Med.* 2020;24(19):10855–10865. doi:10.1111/jcmm.15633
38. Zhang Y, Zeng Y. Curcumin reduces inflammation in knee osteoarthritis rats through blocking TLR4/MyD88/NF-κB signal pathway. *Drug Dev Res.* 2019;80(3):353–359. doi:10.1002/ddr.21538
39. Molnar V, Matišić V, Kodvanj I, et al. Cytokines and chemokines involved in osteoarthritis pathogenesis. *Int J Mol Sci.* 2021;22(17):9208. doi:10.3390/ijms22179208
40. Li M, Yin H, Yan Z, et al. The immune microenvironment in cartilage injury and repair. *Acta Biomater.* 2022;140:23–42. doi:10.1016/j.actbio.2021.12.003
41. Guan T, Ding LG, Lu BY, et al. Combined administration of curcumin and chondroitin sulfate alleviates cartilage injury and inflammation via NF-κB pathway in knee osteoarthritis rats. *Front Pharmacol.* 2022;13:882304. doi:10.3389/fphar.2022.882304
42. Chang B, Hu Z, Chen L, et al. Development and validation of cuproptosis-related genes in synovitis during osteoarthritis progress. *Front Immunol.* 2023;14:1090596. doi:10.3389/fimmu.2023.1090596
43. Bellido M, Lugo L, Roman-Blas JA, et al. Subchondral bone microstructural damage by increased remodelling aggravates experimental osteoarthritis preceded by osteoporosis. *Arthritis Res Ther.* 2010;12(4):R152. doi:10.1186/ar3103

Journal of Inflammation Research

Dovepress

## Publish your work in this journal

The Journal of Inflammation Research is an international, peer-reviewed open-access journal that welcomes laboratory and clinical findings on the molecular basis, cell biology and pharmacology of inflammation including original research, reviews, symposium reports, hypothesis formation and commentaries on: acute/chronic inflammation; mediators of inflammation; cellular processes; molecular mechanisms; pharmacology and novel anti-inflammatory drugs; clinical conditions involving inflammation. The manuscript management system is completely online and includes a very quick and fair peer-review system. Visit <http://www.dovepress.com/testimonials.php> to read real quotes from published authors.

Submit your manuscript here: <https://www.dovepress.com/journal-of-inflammation-research-journal>